A New Analytical Model for Reinforced Concrete Beam-Column Joints Subjected to Cyclic Loading

T. Saito
Kanagawa University, Japan

M. Kikuchi
Hokkaido University, Japan

SUMMARY:
A new beam-column joint finite element model is presented for the non-linear analysis of reinforced concrete (RC) frames. The proposed model captures the bond-slip of reinforcement and shear deformations of the beam-column joint zone to represent the behavior of RC beam-column joints under cyclic loading. The main objective of the present paper is to use the analytical RC frame model to evaluate the influence of joint behavior on the overall performance of RC frames. Comparison of the analytical and test results reveals that the proposed beam-column joint model can reproduce well the fundamental characteristics of non-linear RC beam-column joint behavior.

Keywords: Finite element method, Beam-column joint, Reinforced concrete frame

1. INTRUDUCTION

Under seismic loading, the deformation of reinforced concrete (RC) frame structures is generally influenced by the behavior of the beam-column joints. In addition, the number of RC buildings that use high-strength materials is increasing. In RC buildings, the beam-column joint stress increases as the cross-section of the RC frame members decreases. In recent years, finite element models have been developed that are capable of describing the non-linear behaviors of RC frame structures. However, most of the analytical studies of RC frames are based on the assumption of an ideal bond between the concrete and the reinforcement, and beam-column joints are generally assumed to be rigid. These assumptions are generally reasonable when the non-linear behavior of joint under cyclic loading is negligible. However, since the importance of considering the beam-column joint behaviors in analysis is increasing, a new analytical model of the beam-column joint that considers joint behavior is necessary.

A number of beam-column joint models that consider joint behavior have been proposed. Ghobarah et al. (1999) modeled the joint element with joint shear and bond-slip deformations using discrete rotational springs and material constitutive models. Elmorsi et al. (2000) proposed a joint model composed of 12 nodes and bar elements connected to each node to simulate the bond-slip of reinforcement embedded in the joint. Lowes et al. (2003) proposed a joint element that has four nodes and a total of 12 degrees of freedom. The element was composed of eight zero-length translational springs to simulate the bond-slip of beam and column longitudinal reinforcement, four zero-length translational shear springs to simulate the interface shear deformations of the joint panel zone and a zero-length rotational spring to simulate the joint shear deformation. However, the analytical method employed in these models utilizes linear elastic beam and column elements. Therefore, it is difficult to deal with the bond-slip behavior of reinforcement embedded in the beam and column through the joint. Limkatanyu et al. (2003) also developed a joint model considering bond-slip response. The model is simple and is composed of two elements and uses a rigid link to connect the elements. However, this model assumes a rigid joint and so is not able to represent joint shear deformations.

In the present paper, a new beam-column joint element for the finite element method, based on the fiber-section model, is proposed in order to model the behavior of an RC beam-column joint under cyclic loading. The new model comprises only a small number of nodes for the joint panel and reinforcement bar elements. The model captures the bond-slip of the reinforcement and shear deformations of the beam-column joint panel zone. The present paper also discusses the material models for concrete and steel and constitutive models for reinforcement bond-slip and joint panel zone shear deformations to accurately reproduce the cyclic, non-linear behavior of beam-column joints. The main objective of the present paper is to use this analytical model to evaluate the influence of joint behavior in the overall performance of RC frames. Simulation analyses were performed and compared with actual test data in order to validate the proposed beam-column joint model. Comparisons of two experimental test results of beam-column joint building subassemblies reveal that the proposed analytical model can accurately predict the test behavior and also well represents the detailed large-deformation, non-linear behaviors of RC beam-column joints.

2. RC BEAM ELEMENT WITH BOND-SLIP

In this section, RC beam elements based on the finite element method for analyzing the behavior of RC frames are discussed. Figure 1 shows the nodal displacements of an RC beam element with bond-slip and the cross-section of the element. The elements are based on the fiber-section model, and the cross-section of element consists of concrete layers and steel layers (total n layers). The element has two nodes and 3 + n degrees of freedom are defined at each node. The nodal displacements: axial displacement, u, transverse displacement, w, rotate displacement, θ, and reinforcement bars slip displacement, s, are also shown in Figure 1. Using the Euler-Bernoulli beam theory, the incremental strain and stress, $\Delta\varepsilon_{ci}$ and $\Delta\sigma_{ci}$, respectively, of an arbitrary concrete layer, i, are given as

$$\Delta\varepsilon_{ci} = \frac{d\Delta u}{dx} - z_{ci}\frac{d^2\Delta w}{dx^2} \tag{2.1}$$

$$\Delta\sigma_{ci} = E_{ci}\Delta\varepsilon_{ci} \tag{2.2}$$

Similarly, the incremental strain and stress, $\Delta\varepsilon_{si}$ and $\Delta\sigma_{si}$, of an arbitrary steel layer, i, are given as

$$\Delta\varepsilon_{si} = \frac{d\Delta u}{dx} - z_{si}\frac{d^2\Delta w}{dx^2} + \frac{d\Delta s_i}{dx} \tag{2.3}$$

$$\Delta\sigma_{si} = E_{si}\Delta\varepsilon_{si} \tag{2.4}$$

where z_{ci} and z_{si} are the distances the between arbitrary concrete and steel layers, i, and the reference axis of the element, and E_{ci} and E_{si} are the stiffnesses of arbitrary concrete and steel layers i.

The relationship between bond stress, τ_{bi}, and slip displacement, s_i, along the anchored bar is assumed to be as follows:

$$\Delta\tau_{bi} = K_{bi}\Delta s_i \tag{2.5}$$

where K_{bi} is the bond stiffness of the arbitrary steel layers, i.

The equilibrium equation for an RC frame element with bond-slip using the principal of minimum potential energy, $\Delta\Pi$, is expressed as follows:

$$\Delta\Pi = (\Delta U_c + \Delta U_s + \Delta U_b) - \Delta V \tag{2.6}$$

where ΔU_c and ΔU_s are the potential energy in the concrete and the steel, respectively, ΔU_b is the potential energy of bond-slip, and ΔV is the potential energy of the external loads.

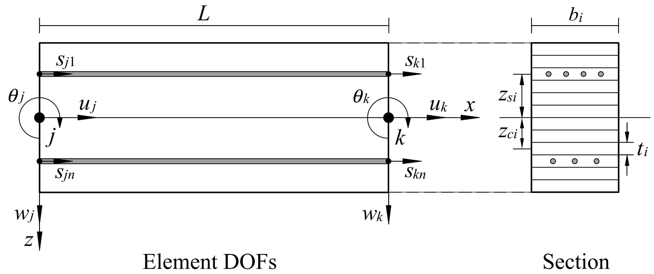

Figure 1. RC frame element with bond-slip

In the finite element method based on the displacement method, the displacements of the element are expressed as functions of the nodal displacements through the displacement shape functions. The displacement shape functions in the element are defined as a linear function of the axial displacement, u, and the reinforcement bond-slip displacement, s, is defined as a cubic function of the transverse displacement, w. Thus, the nodal displacements are grouped into element displacement vectors, $\{\Delta u\}$, $\{\Delta w\}$, and $\{\Delta s\}$, which are defined as follows:

$$\{\Delta u\} = \{\Delta u_j \ \Delta u_k\}^T \tag{2.7}$$

$$\{\Delta w\} = \{\Delta w_j \ \Delta\theta_j \ \Delta w_k \ \Delta\theta_k\}^T \tag{2.8}$$

$$\{\Delta s\} = \{\Delta s_j \ \Delta s_k\}^T \tag{2.9}$$

where θ is the rotation displacement of each node and is expressed as $\theta = \frac{dw}{dx}$.

The following finite element equation for a beam element with bond-slip is derived by substituting Eqns. 2.1 through 2.5 into Eqn. 2.6:

$$\begin{bmatrix} K_{uu} & K_{uw} & K_{us} \\ & K_{ww} & K_{ws} \\ sym. & & K_{ss} \end{bmatrix} \begin{Bmatrix} \Delta u \\ \Delta w \\ \Delta s \end{Bmatrix} = \begin{Bmatrix} \Delta P_u \\ \Delta P_w \\ \Delta P_s \end{Bmatrix} \tag{2.10}$$

where $[K]$ is the element stiffness matrix corresponding to the element displacement vectors, and $\{\Delta P\}$ is the element force vector corresponding to the element displacement vector.
The basic component of the analytical model for the RC frame used in the present study is a simple RC beam and column model composed of RC beam and column elements.

3. RC BEAM-COLUMN JOINT MODEL

Figure 2 shows the new RC beam-column joint element with the bond-slip of reinforcement and shear deformations of the beam-column joint panel zone. The joint element consists of a beam element and a column element. The nodal degrees of freedom of this element are similar to those of the beam and column elements. Therefore, the joint element can easily be connected to the beam and the column elements in the model, the frame model consisting of these elements can represent the reinforcement slip behavior embedded in the beam and column and through the joint. Figure also shows the displacement field of the joint element. The element has four nodes, l, r, b, and t. The subscripts in figure indicate the node. It is assumed that the joint panel can deform uniformly in shear, and the shear strain of the joint element is expressed as a combination of the horizontal shear displacement, u_{jp}, and the vertical shear displacement, w_{jp}. Thus, the incremental joint shear strain, $\Delta\gamma$, can be calculated using the following equation:

$$\Delta\gamma = \frac{d\Delta u_{jp}}{dz} + \frac{d\Delta w_{jp}}{dx} = \frac{\Delta u_b - \Delta u_t}{H} + \frac{\Delta w_r - \Delta w_l}{W} \tag{3.1}$$

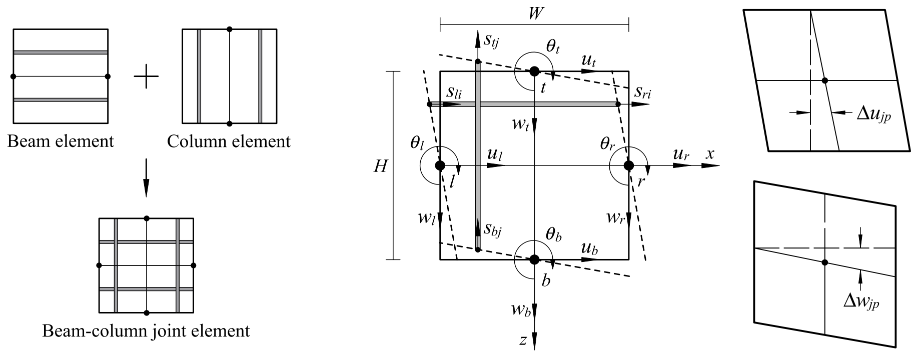

Figure 2. A new beam-column joint element

where H is height of the joint element, and W is width of the joint element.

Furthermore, it is necessary to define the transformation of nodal displacements in order to express the incremental joint shear strain relationship of Eqn. 3.1. The equations for the transformation of nodal displacements are expressed through the geometrical relationships of the deformations in Figure 3, as follows:

$$\left.\begin{aligned}
&\Delta u_l - \frac{\Delta u_b}{2} - \frac{\Delta u_t}{2} = \Delta u_l' = 0\\
&\Delta u_r - \frac{\Delta u_b}{2} - \frac{\Delta u_t}{2} = \Delta u_r' = 0\\
&\Delta \theta_l + \frac{\Delta u_b}{H} - \frac{\Delta u_t}{H} = \Delta \theta_l' = 0\\
&\Delta \theta_r + \frac{\Delta u_b}{H} - \frac{\Delta u_t}{H} = \Delta \theta_r' = 0\\
&\Delta w_b - \frac{\Delta w_l}{2} - \frac{\Delta w_r}{2} = \Delta w_b' = 0\\
&\Delta w_t - \frac{\Delta w_l}{2} - \frac{\Delta w_r}{2} = \Delta w_t' = 0\\
&\Delta \theta_b + \frac{\Delta w_l}{W} - \frac{\Delta w_r}{W} = \Delta \theta_b' = 0\\
&\Delta \theta_t + \frac{\Delta w_l}{W} - \frac{\Delta w_r}{W} = \Delta \theta_t' = 0
\end{aligned}\right\} \tag{3.2}$$

These equations are formulated into the following matrix equation:

$$\begin{Bmatrix} \Delta_l' \\ \Delta_r' \\ \Delta_b' \\ \Delta_t' \end{Bmatrix} = \begin{bmatrix} I & O & T_b & T_t \\ O & I & T_b & T_t \\ T_l & T_r & I & O \\ T_l & T_r & O & I \end{bmatrix} \begin{Bmatrix} \Delta_l \\ \Delta_r \\ \Delta_b \\ \Delta_t \end{Bmatrix} \tag{3.3}$$

where

$$\{\Delta_l\} = \{\Delta u_l \quad \Delta w_l \quad \Delta\theta_l \quad \Delta s_{il}\}^T \qquad \{\Delta_l'\} = \{\Delta u_l' \quad \Delta w_l \quad \Delta\theta_l \quad \Delta s_{il}\}^T$$

$$\{\Delta_r\} = \{\Delta u_r \quad \Delta w_r \quad \Delta\theta_r \quad \Delta s_{ir}\}^T \qquad \{\Delta_r'\} = \{\Delta u_r' \quad \Delta w_r \quad \Delta\theta_r \quad \Delta s_{ir}\}^T$$

$$\{\Delta_b\} = \{\Delta u_b \quad \Delta w_b \quad \Delta\theta_b \quad \Delta s_{ib}\}^T \qquad \{\Delta_b'\} = \{\Delta u_b \quad \Delta w_b' \quad \Delta\theta_b \quad \Delta s_{ib}\}^T$$

$$\{\Delta_t\} = \{\Delta u_t \quad \Delta w_t \quad \Delta\theta_t \quad \Delta s_{it}\}^T \qquad \{\Delta_t'\} = \{\Delta u_t \quad \Delta w_t' \quad \Delta\theta_t \quad \Delta s_{it}\}^T$$

$$[T_l] = \begin{bmatrix} 0 & 0 & 0 & 0 \\ 0 & -\frac{1}{2} & 0 & 0 \\ 0 & \frac{1}{W} & 0 & 0 \\ 0 & 0 & 0 & 0 \end{bmatrix} \quad [T_r] = \begin{bmatrix} 0 & 0 & 0 & 0 \\ 0 & -\frac{1}{2} & 0 & 0 \\ 0 & -\frac{1}{W} & 0 & 0 \\ 0 & 0 & 0 & 0 \end{bmatrix} \quad [T_b] = \begin{bmatrix} -\frac{1}{2} & 0 & 0 & 0 \\ 0 & 0 & 0 & 0 \\ \frac{1}{H} & 0 & 0 & 0 \\ 0 & 0 & 0 & 0 \end{bmatrix} \quad [T_t] = \begin{bmatrix} -\frac{1}{2} & 0 & 0 & 0 \\ 0 & 0 & 0 & 0 \\ -\frac{1}{H} & 0 & 0 & 0 \\ 0 & 0 & 0 & 0 \end{bmatrix}$$

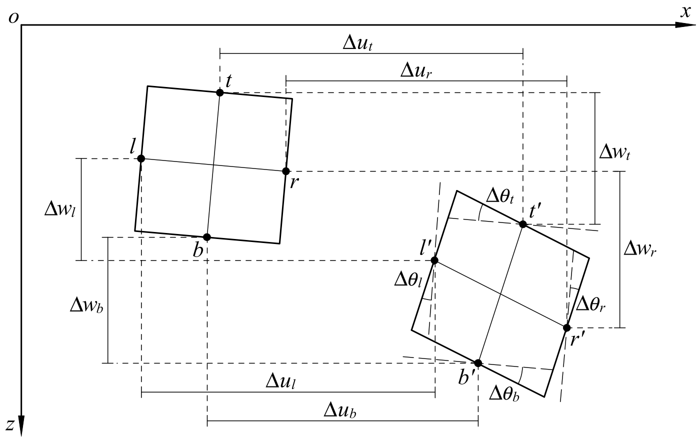

Figure 3. Beam-column joint element incremental nodal displacements

where $[I]$ is the identity matrix, $[O]$ is the null matrix, and the vector and matrix subscripts l, r, b, and t refer to the individual nodes of the joint element.
Eqn. 3.3 can be rewritten as follows:

$$\{\Delta'_{jp}\} = [T_{jp}]\{\Delta_{jp}\} \tag{3.4}$$

where $\{\Delta'_{jp}\}$ are the transformed displacement vectors in the joint element, $[T_{jp}]$ is the transformation matrix of the joint element, and $\{\Delta_{jp}\}$ are the displacement vectors of the joint element. In order to adapt these relationships for analysis, the following matrix equation is derived using Eqn. 3.4 and the finite element equation of the joint element:

$$[T_{jp}^{-1}]^T [K_{jp}] [T_{jp}^{-1}] \{\Delta'_{jp}\} = [T_{jp}^{-1}]^T \{\Delta P_{jp}\} \tag{3.5}$$

where $[K_{jp}]$ is the stiffness matrix of the joint element, $\{\Delta P_{jp}\}$ are the force vectors of the joint element, and Eqn. 3.5 is the finite element equation of the joint element transformed displacements. This equation requires a boundary condition such that the displacements defined according to Eqn. 3.2 are zero, in order to satisfy the relationship of Eqn. 3.1. Thus, with the zero-displacement boundary condition and solving Eqn. 3.5, joint displacements that include panel zone shear deformations are obtained.

4. MATERIAL MODEL

In this section, the material models for concrete, steel, bond-slip of reinforcement, and joint shear deformation are discussed. Figure 4 shows the material models used in the present study.

4.1. Concrete Material Model

Figure 4(a) shows the concrete material stress-strain relationship used in the present study. For the tension monotonic envelope, a linear stress-strain relationship up to cracking is assumed. After cracking, a multi-linear, two-stage stress reduction is used to define the tension degradation. In compression, the model is based on the Saenz equation up to the compressive strength, beyond which a linear descending branch represents compression softening.

4.2. Steel Material Model

The steel material stress-strain relationship is shown Figure 4(b). For a monotonic response, a bi-linear model is used for the stress-strain relationships. For hysteretic response, the Menegotto-Pinto model is

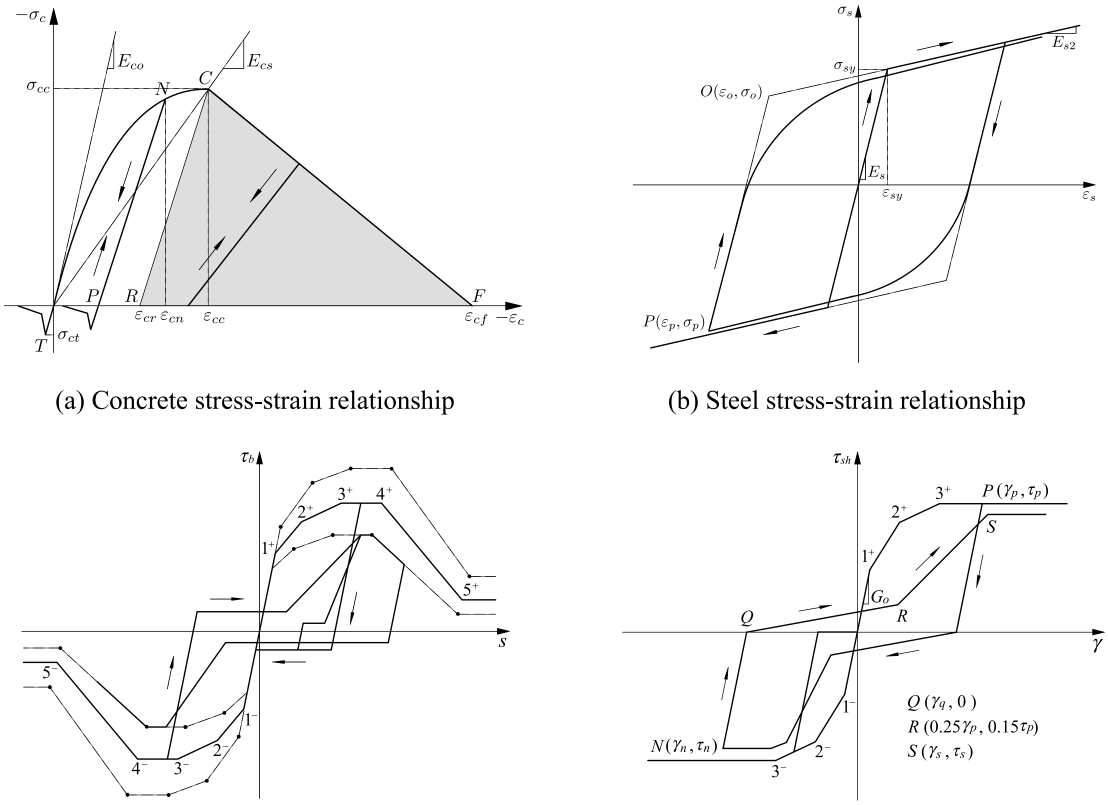

(a) Concrete stress-strain relationship

(b) Steel stress-strain relationship

(c) Bond-slip stress-deformation relationship

(d) Joint shear stress-strain relationship

Figure 4. Material and constitutive models

used to represent the Bauschinger effect of the steel material. The curve from the point of load reversal, P, is expressed as follows:

$$\sigma^* = R_s \varepsilon^* + \frac{(1-R_s)\varepsilon^*}{(1+\varepsilon^{*R_b})^{1/R_b}} \tag{4.1}$$

where

$$\sigma^* = \frac{\sigma_s - \sigma_p}{\sigma_o - \sigma_p} \qquad \varepsilon^* = \frac{\varepsilon_s - \varepsilon_p}{\varepsilon_o - \varepsilon_p} \qquad R_s = \frac{E_{s2}}{E_s}$$

R_s is the strain hardening factor, R_b is the Bauschinger effect factor, E_s is the reinforcement elastic modulus, and E_{s2} is the post-yield modulus of reinforcement.

4.3. Reinforcement Bond-slip Model

The monotonic envelope of the bond stress-slip material model consists of five specific points (Figure 4(c)). The bond stress and slip of each point are determined according to the bond strength, τ_3, and the slip deformation, s_3. In addition, the bond strength may change due to various factors related to the bond stress. Therefore, in the present study, we use the bond strength relationship proposed by Lowes et al. (2004). The bond strength, τ_3, and slip, s_3, are expressed as follows:

$$\tau_3 = \alpha_1 \cdot \alpha_2 \cdot \alpha_3 \cdot \alpha_4 \cdot \alpha_5 \cdot \tau_3' \;\; [N/mm^2] \tag{4.2}$$

$$s_3 = \tau_3 / 20.0 \;\; [mm] \tag{4.3}$$

where α_1, α_2, α_3, α_4, and α_5, are the coefficients expressing the influence of the bond stress, and τ'_3 is the basic bond strength.

Furthermore, the unloading and reloading paths are based on the model developed by Morita et al. (1975). Figure 6(c) shows the typical unloading and reloading paths that start from the monotonic envelope.

4.4. Joint Shear Model

The constitutive model developed by Lowes et al. (2003) is used (Figure 4(d)). For defining the monotonic envelope of the joint shear stress-strain relationship, it is necessary to perform a preliminary analysis, which uses the modified compression field theory (MCFT) proposed by Vecchio et al. (1986). This analytical method computes the monotonic envelope of reinforced concrete shear behavior using the joint geometry, the material properties, and the reinforcing steel ratio. In addition, unloading and reloading paths are modeled in order to express the damage of the joint member associated with the deterioration of shear strength and stiffness on the reloading path. In the present study, the unloading stiffness is assumed to be the initial stiffness.

5. NUMERICAL VERIFICATION OF THE PROPOSED BEAM-COLUMN JOINT MODEL

In this section, comparisons of the results obtained using the proposed beam-column joint model with experimental data are presented. The verifications are performed based on the results of an experimental test of RC frame subassemblies.

Jiang and Kitayama (1996) tested a series of interior RC beam-column subassemblies. In their study, one of these subassemblies, labeled specimen M1, is selected to confirm the validity of the proposed beam-column joint model. Figure 5 shows the configuration of specimen M1. Following the original research by Jiang and Kitayama, the specimen has two joints in the frame. The beam and column cross-sections and the material properties are also shown in Figure 5. The lower end of each column is a pin support, and the beam ends are pin-roller supported. The upper ends of the columns were subjected to repeated cyclic loading: one cycle at a story drift angle of 1/400 rad and two cycles at story drift angles of 1/200 rad, 1/100 rad, 1/50 rad, and 1/25 rad. During the test loading history, the inelastic actions occurred mostly around the joints.

Numerical models were developed to simulate the response of the Jiang and Kitayama test specimen to the test loading. The element axial length is set to 100 mm. Each outer beam and each column is represented by seven elements. The central beam is represented by 14 elements. The cross-sections of the beam and column elements are divided into 51 fiber layers. The proposed joint model connects the beam and column elements and creates the overall model of the RC frame. Each element was modeled using the material, geometric, and design parameters provided by the Jiang and Kitayama test data. The loading sequence used for the analysis is reversed cyclic loading using displacement control, which is the same as for the experimental test.

Figure 6 compares the experimental and numerical results. This figure shows the test results and the analytical results, including both the reinforcement bond-slip and joint shear deformations. In addition, the analytical Cases 1 and 2 results are also shown in order to clarify the influence of beam-column joint behavior on the performance of the entire RC frame in the analysis.

Case 1: Only bond-slip of reinforcements is considered (without joint shear deformation)
Case 2: Only joint shear deformation is considered (without bond-slip of reinforcements)

The comparisons reveal that the proposed model can capture the experimental load-displacement relationship, but slightly overestimates the unloading stiffness. In particular, comparison with the test results reveals that the analytical results can represent well the fundamental characteristics of the test results, which show the behavior in terms of both energy dissipation and the pinching effect caused by bond-slip and joint shear behavior in the beam-column joint. On the other hand, the results for Cases 1 and 2 show that the beam-column joint behaviors do not indicate that the hysteretic energy absorption

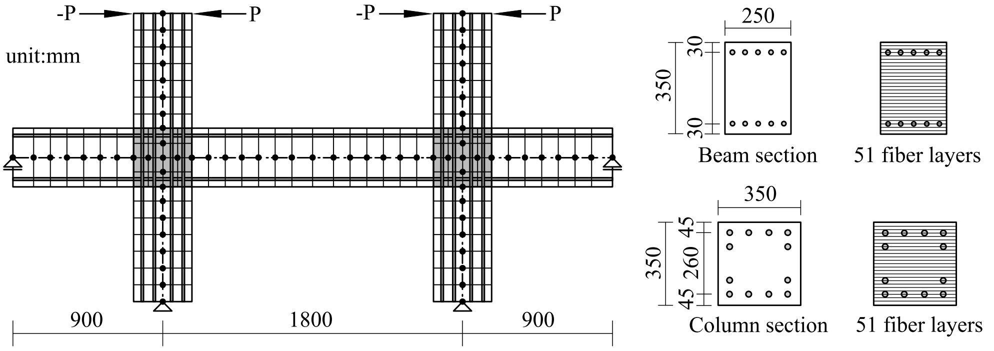

Concrete	Beam reinforcement	Column reinforcement
$E_{co} = 44500\,N/mm^2$	$E_s = 188100\,N/mm^2$	$E_s = 193200\,N/mm^2$
$\sigma_{cc} = -44.50\,N/mm^2$	$E_{s2} = 1881\,N/mm^2$	$E_{s2} = 1932\,N/mm^2$
$\sigma_{ct} = 3.35\,N/mm^2$	$\sigma_{sy} = 346.1\,N/mm^2$	$\sigma_{sy} = 363.2\,N/mm^2$
$\varepsilon_{cc} = -0.20\,\%$	$\varepsilon_{sy} = 0.184\,\%$	$\varepsilon_{sy} = 0.188\,\%$

Beam	Number of all elements : 28 Element axial length : 100mm
Column	Number of all elements : 14 Element axial length : 100mm

Figure 5. RC beam-column joint subassemblies tested by Jiang and Kitayama (specimen M1)

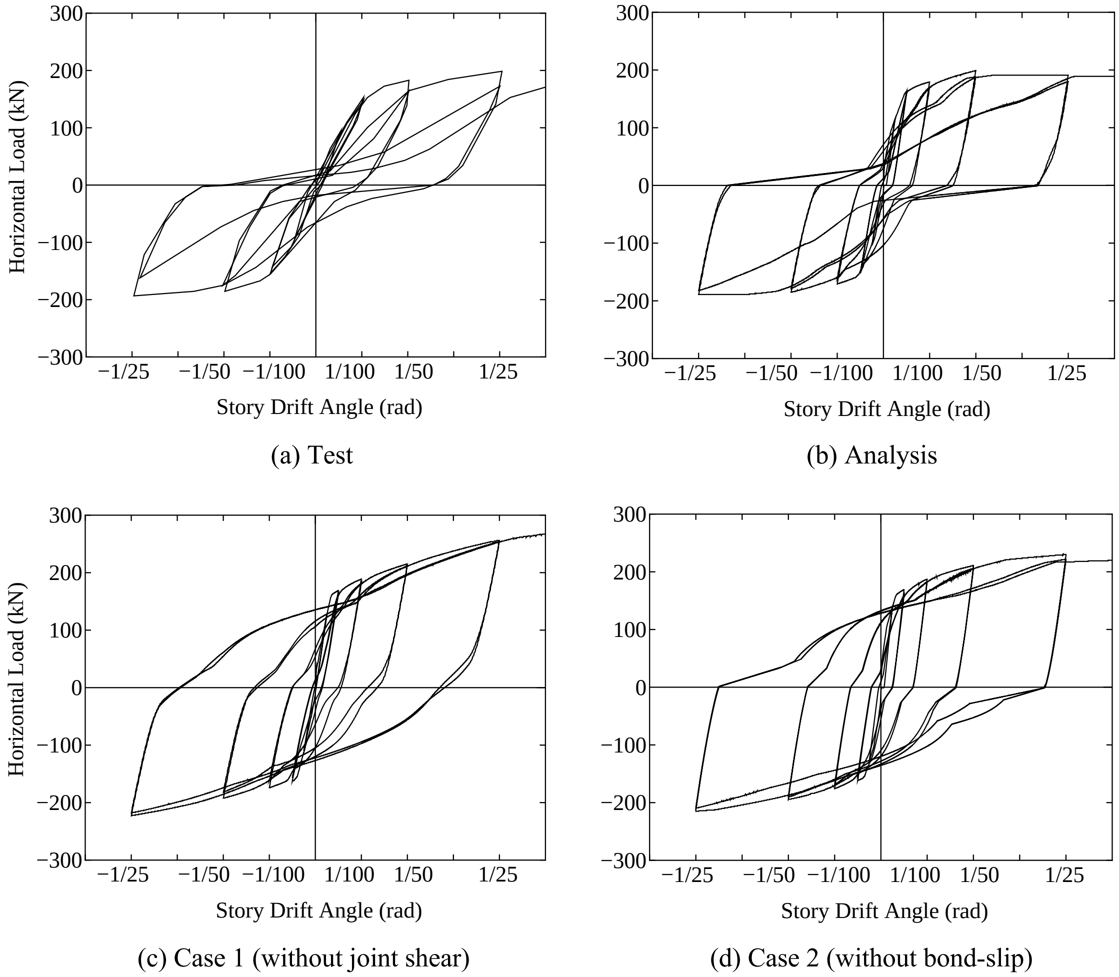

Figure 6. Test and analytical results of test specimen M1 reported by Jiang and Kitayama

is significantly overestimated. The behavior of both cases is similar until a story drift angle 1/200 (rad). However, the cases are not able to re-produce the actual test beyond a story drift angle of approximately 1/100 (rad). The differences between the numerical results reveal that it is essential to consider the joint behavior, i.e., the bond-slip of reinforcements embedded through the joint and the shear deformation of the joint panel, for the accurate analysis of the non-linear behavior of RC frame structures.

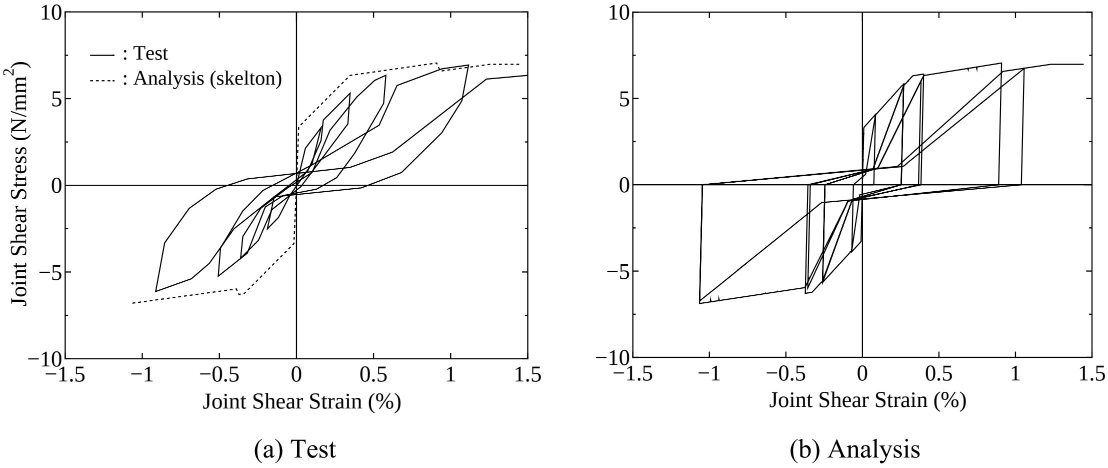

Figure 7. Comparisons of joint shear stress versus joint shear strain

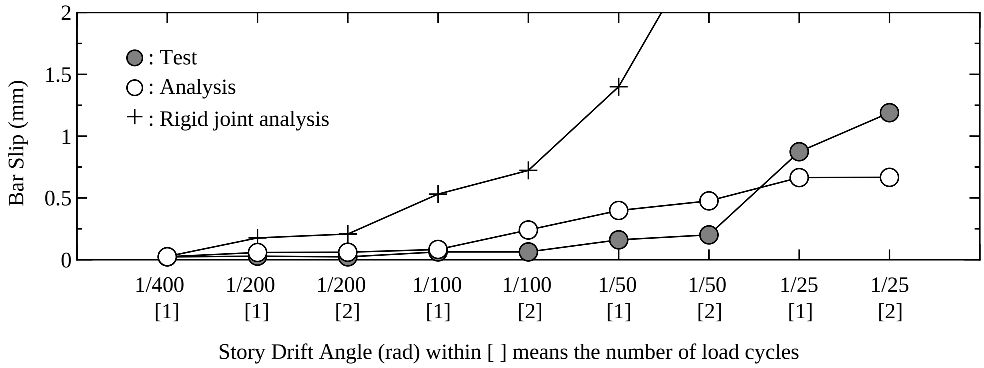

Figure 8. Comparisons of reinforcement top bar slip at the center of the beam-column joint

Jiang and Kitayama monitored the joint shear strain by measuring the deformation along the diagonal of the joint. Figure 7 compares the test and analytical joint shear stress versus shear strain relations. The skeleton curve of analysis calculated using the MCFT shows good agreement with the test results. However, since the mode in the present study assumes that the unloading stiffness is equal to the initial stiffness, the analytical unloading stiffness is higher than the test stiffness. The high unloading stiffness of the joint shear behavior may cause an overestimation of the energy absorption of the RC frame analytical response. Consequently, in the future, we intend to improve the modeling of the unloading stiffness behavior. However, the shear strain level of each load cycle computed by the proposed joint model is in fair agreement with test results. Therefore, this result reveals that the new joint model can reproduce well the shear behavior of the beam-column joint panel in the RC frame structure.

Figure 8 compares the test and analytical reinforcement top bar slip at the center of the beam-column joint. The horizontal axis indicates the loading cycles at the time of peak positive loading. This figure also shows the analytical result assuming no joint shear deformation. The analytical response with joint shear deformation shows quite good agreement with the test response. Both results for the reinforcement bar slip are contained within the range of approximately one millimeter. In contrast, the rigid joint analytical result significantly overestimates reinforcement bar slip as early as a story drift angle of 1/100 rad. The results clearly indicate the contribution of beam-column joint shear deformation to reinforcement bar-slip. In general, joint shear deformation results in a reduction in the beam and column hinge inelastic responses. As such, the reinforcement bar-slip may be reduced by the reduction in beam and column deformations.

6. CONCLUSION

A new beam-column joint model for large-deformation, non-linear behavior of reinforced concrete frames under cyclic loading has been developed. The new model consists of a multi-node joint panel zone and reinforcing bar elements. The model captures the bond-slip of reinforcement and shear behaviors of the beam-column joint. Simulation analyses were performed and compared with actual test data to validate the proposed beam-column joint model. Comparisons of the responses for an experimental test of beam-column joint building subassemblies reveal that the analytical model using the new simple beam-column joint element can accurately predict the test behavior and well represents the detailed large-deformation, non-linear behaviors of RC beam-column joints. And comparisons of the analytical and test results reveals that the proposed beam-column joint model can reproduce well the fundamental characteristics of non-linear cyclic RC beam-column joint behavior in terms of both energy dissipation and pinching effect caused by bond-slip and joint shear behavior in the beam-column joint. If bond-slip and joint shear deformations are not considered, then the hysteretic energy absorption is significantly overestimated.

REFERENCES

Elmorsi, M., Kianoush, M.R., Tso, W.K. (2000) Modeling bond-slip deformations in reinforced concrete beam-column joints. *Canadian Journal of Civil Engineering* **27**, 490-505.

Ghobarah, A., Biddah, A. (1999) Dynamic analysis of reinforced concrete frames including joint shear deformation. *Engineering Structures* **21**, 971-987.

Jiang, Z., Kitayama, K. (1996) Beam-column joint shear and beam longitudinal bars in reinforced concrete frames. *Journal of Structural Engineering* **42B**, 169-179. (in Japanese)

Limkatanyu, S., Spacone, E. (2003) Effects of reinforcement slippage on the nonlinear response under cyclic loadings of RC frame structures. *Earthquake Engineering and Structural Dynamics* **32**, 2407-2424.

Lowes, L.N., Altoontash, A. (2003) Modeling reinforced-concrete beam-column joints subjected to cyclic loading. *Journal of Structural Engineering* **129**, 1686-1697.

Lowes, L.N., Moehle, J.P., Govindjee, S. (2004) Concrete-steel bond model for use in finite element modeling of reinforced concrete structures. *ACI Structural Journal* **101**, 501-511.

Morita, S., Kado, T. (1975) Bond-slip relationship under repeated loading. *Transactions of the Architectural Institute of Japan* **229**, 15-24. (in Japanese)

Vecchio, F.J., Collins, M.P. (1986) The modified-compression field theory for reinforced-concrete elements subjected shear. *ACI Journal* **83**, 219-231.